

Electronic structure of small band gap oligomers based on cyclopentadithiophenes and acceptor units†‡

Bram P. Karsten,^a Johannes C. Bijleveld,^a Lucas Viani,^b Jérôme Cornil,^b Johannes Gierschner^{bc} and René A. J. Janssen^{*a}

Received 21st January 2009, Accepted 24th March 2009

First published as an Advance Article on the web 28th April 2009

DOI: 10.1039/b901374a

A combined experimental and theoretical study is presented on a series of well-defined small band gap oligomers. These oligomers comprise two terminal electron-rich cyclopentadithiophene units connected to six different electron deficient aromatic rings that allow tuning the optical band gap from 1.4 to 2.0 eV. Optical absorptions of the ground state, triplet excited state, and radical cation have been investigated. The optical band gaps correlate with the electrochemical oxidation and reduction potentials and are further supported by quantum-chemical calculations at the density functional theory (DFT) level. The optical absorptions of the radical cations show only little variations among the different oligomers, suggesting that the charge is mainly localized on the donor moieties. Triplet energy levels are generally low (<1.2 eV) and the singlet–triplet splitting remains significant when going to smaller band gaps.

Introduction

Polymer solar cells are an attractive means for converting sunlight directly into electricity. Due to their flexibility, ease of processing and their potential low cost, polymer solar cells could become viable candidates for replacing the current energy resources. In recent years, tremendous advances have been made in increasing the efficiency of solar cells containing polymers like poly(3-hexylthiophene).^{1–3} The photocurrent in these devices is, however, limited by the poor overlap between the spectrum of the sun and the absorption spectrum of these polymers.⁴ This poor spectral overlap results in the loss of a large fraction of the energy contained in the sunlight, because photons with energies below *ca.* 2 eV are not absorbed. This is by far the largest fraction of the light emitted by the sun.

To increase spectral overlap, reducing the band gap of π -conjugated polymers is necessary. Hence, high-efficiency organic solar cells will consist, at least partly, of small band gap polymers. To date, several soluble conjugated polymers with reduced band gaps have been reported,^{5–16} yielding energy conversion efficiencies up to 5.5% under simulated solar light in combination with fullerene acceptors.¹⁴ Various approaches to small band gap polymers exist, *e.g.* poly(isothianaphthene)^{17,18} and poly(thieno[3,4-*b*]pyrazine),^{19,20} polyanthrylenebutadiynylenes,²¹ and

cross-conjugated polymers such as polyindeno[1,2-*b*]fluorene.²² A versatile approach to reduce the band gaps of conjugated polymers is to incorporate segments with alternating electron rich donor and electron deficient acceptor units in the polymer backbone.^{23–33} As donor segments, generally oligothiophene units, or more recently bridged derivatives, such as cyclopentadithiophene,^{11,14,16,34–39} have been employed. Acceptor units vary, but benzothiadiazole and thienopyrazine have been found to be useful.

Detailed understanding of the electrochemical and optical properties of short oligomers of small band gap polymers will help gain valuable insight into the design rules for new materials and into the processes limiting the efficiency of polymer solar cells. In this respect we note that using thiophene-thienopyrazine based small band gap oligomers, we could demonstrate that the number of acceptor units in the oligomer is a crucial factor that outweighs the importance of extended alternating donor–acceptor conjugation in determining the optical gap.^{40–42} The successful design of new polymers with optimized properties for solar energy conversion will not merely depend on the band gap and HOMO and LUMO levels, but also the triplet energy level. It has been shown that recombination of photogenerated charges into a low-lying triplet state may occur when the energy of the triplet state is below that of the charge transfer state.^{43,44} In fact, triplet recombination might be an important loss mechanism.⁴⁵ So far, however, very little is known about the exchange energy and the triplet energy level in small band gap polymers, and whether it scales differently with singlet excited state energy than in traditional conjugated polymers.^{46,47}

In this paper, we investigate the influence of the nature of the acceptor unit on the optical and electrochemical properties of oligomeric small band gap systems. Oligomers consisting of two cyclopentadithiophene units and six different acceptor units have been synthesized. Their optical absorption spectra, oxidation and reduction potentials, triplet absorptions and triplet energy

^aLaboratory of Macromolecular and Organic Chemistry, Eindhoven University of Technology, P.O. Box 513, NL-5600, MB, Eindhoven, The Netherlands. E-mail: r.a.j.janssen@tue.nl

^bLaboratory for Chemistry of Novel Materials, University of Mons-Hainaut, Place du Parc 20, B-7000 Mons, Belgium

^cMadrid Institute of Advanced Studies (IMDEA-Nanoscience) UAM, Faculty of Science Module C-IX, 3rd Level, Av. Tomás y Valiente, 7 Campus Cantoblanco, E-28049 Madrid, Spain

† This paper is part of a Journal of Materials Chemistry theme issue on solar cells. Guest editors: Michael Grätzel and René Janssen.

‡ Electronic supplementary information (ESI) available: Detailed synthetic procedures. See DOI: 10.1039/b901374a

levels, and corresponding radical cations were investigated in detail. The results are rationalized by density functional theory (DFT) calculations. Clear correlations between the nature of the acceptor and the band gap and the HOMO and LUMO levels have been found. The energy of the triplet excited state of the systems under study has been found to be lower than 1.2 eV.

Experimental

Detailed synthetic procedures are given in the ESI.† UV/vis spectra were recorded on a Perkin Elmer Lambda 900 UV/vis/NIR spectrometer. Cyclic voltammograms were recorded in an inert atmosphere with 0.1 M tetrabutyl ammonium hexafluorophosphate (TBAPF₆) in dichloromethane as supporting electrolyte. The working electrode was a platinum disc (0.2 cm²) and the counter electrode was a silver electrode. The samples were measured using an Ag/AgCl reference electrode with Fc/Fc⁺ as an internal standard using a μAutolab II with a PGSTAT30 potentiostat. PIA spectra were recorded by exciting with a mechanically modulated cw Ar-ion laser ($\lambda = 351$ and 364 nm, 275 Hz) pump beam and monitoring the resulting change in transmission of a tungsten-halogen probe light through the sample (ΔT) with a phase-sensitive lock-in amplifier after dispersion by a grating monochromator and detection, using Si, InGaAs, and cooled InSb detectors. The pump power incident on the sample was typically 25 mW with a beam diameter of 2 mm. The PIA ($\Delta T/T$) was corrected for the photoluminescence, which was recorded in a separate experiment. Photoinduced absorption spectra and photoluminescence spectra were recorded with the pump beam in a direction almost parallel to the direction of the probe beam. The solutions were studied in a 1 mm near-IR grade quartz cell at room temperature.

Results and discussion

Synthesis

The oligomers were synthesized according to Scheme 1. 4,4-Bis(2-ethylhexyl)cyclopentadithiophene (CPDT, **1**) was transformed into its boronic ester **2** and tributylstannyl derivative **3**. Oligomers with a phenyl-based acceptor (quinoxaline (**Q**), benzothiadiazole (**BT**) and benzoxadiazole (**BO**)) were then prepared by Suzuki coupling of boronic ester **2** with the dibromo-derivative of the acceptor. Tributylstannyl derivative **3** was reacted with 2,5-dibromo-3,4-dinitrothiophene (**7**) and the nitro groups were reduced with tin(II) chloride, to give diamine **9**. The oligomers with a thiophene-based acceptor (thienopyrazine (**TP-a**), acenaphthothienopyrazine (**TP-b**) and thienothiadiazole (**TT**)) were formed by reaction of **9** with a diketone to give **TP-a** and **TP-b**, or with *N*-thionylaniline to give **TT**. All oligomers were characterized by NMR, IR, and MALDI-TOF mass spectrometry.

Electrochemical and optical properties

The redox properties of the oligomers were investigated by cyclic voltammetry (Fig. 1). The onsets of oxidation (E_{ox}) and reduction (E_{red}) waves determined from the voltammograms and the electrochemical band gap (E_g^{cv}), defined as their difference, are summarized in Table 1. From these data it can be seen that the

nature of the central unit has a major effect on the oxidation and reduction potentials. Changing the acceptor system from a benzene-based (**Q**, **BT** and **BO**) to a thiophene-based (**TP-a**, **TP-b** and **TT**) central unit significantly lowers the oxidation potential. This implies that the HOMO levels of the latter systems are higher in energy, which gives rise to lower open circuit voltages in solar cells, made of polymers using thienopyrazine and thienothiadiazole. The potential difference between the first and second oxidation waves for **Q**, **BT**, and **BO** is ~ 200 mV and significantly less than the ~ 300 mV splitting for **TP-a**, **TP-b** and **TT**. This indicates that the Coulomb interaction between the two positive charges is stronger for the thiophene based systems and signifies the stronger conjugation of the two CPDT units *via* the central unit in this case. At the same time the oligomers with a thiophene-based central unit (**TP-a**, **TP-b**, and **TT**) also cause a lower (*i.e.* less negative) reduction potential. This is most clear by comparing the reduction potentials of **Q** and **TP-a** that both have a pyrazine ring or comparing **BT** and **TT** that both have a thiadiazole ring.

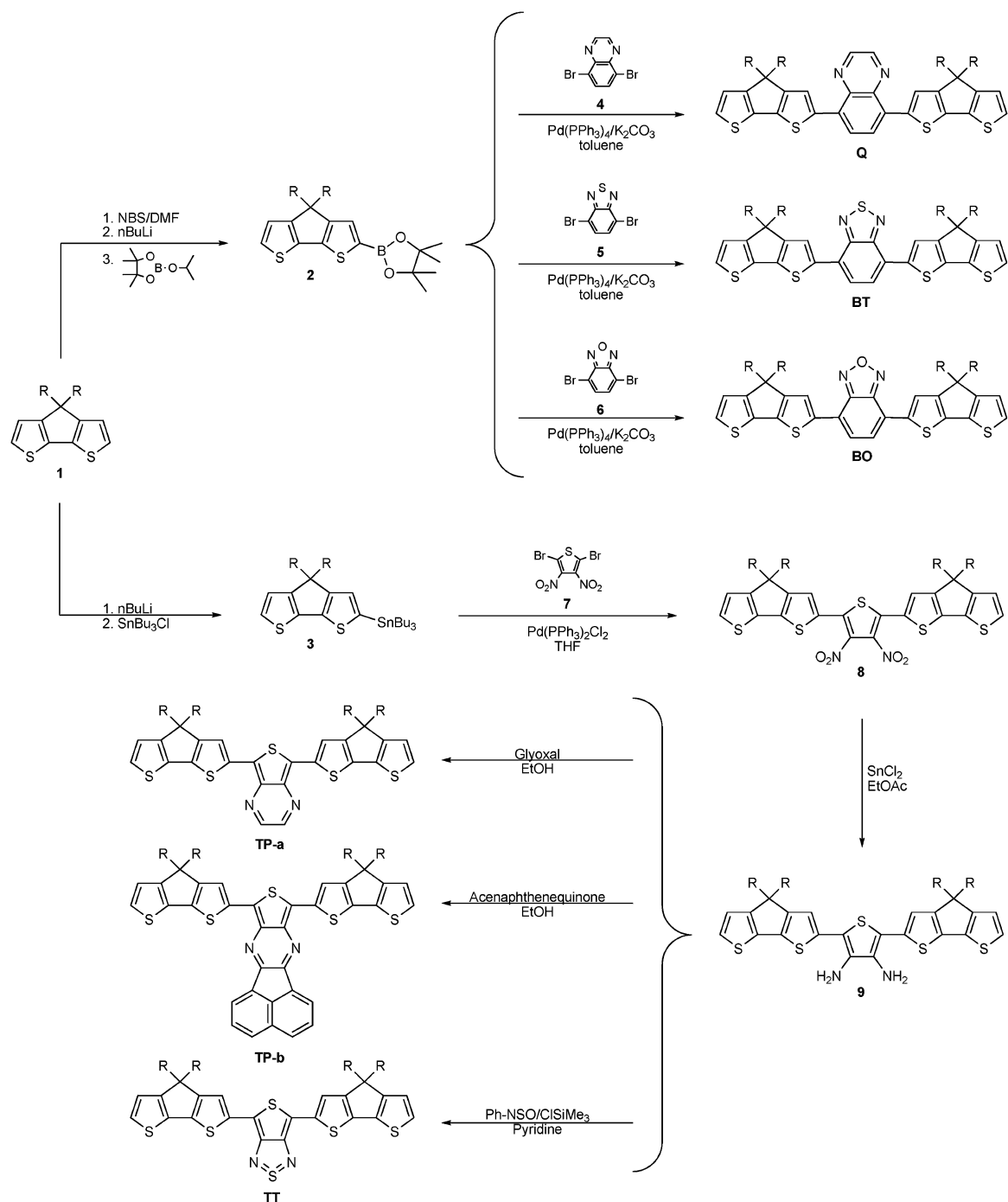
In this series of oligomers **BO** deviates from the other compounds by its increased oxidation potential. Although the band gap is almost equal to **BT**, the redox potentials are raised by almost 0.1 V, making benzoxadiazole an attractive alternative to the commonly used benzothiadiazole for use in small band gap polymer solar cells, because of the expected higher open-circuit voltages.

The UV/vis absorption spectra of the oligomers in toluene are depicted in Fig. 2. The optical band gap E_g^{opt} (calculated from the absorption onset) and electrochemical band gap (E_g^{cv}) are virtually identical (Table 1), the maximum difference being 0.06 eV within experimental error. The onset of absorption shifts from 2.02 eV for **Q** to 1.95 eV for **BT** and **BO**. Replacing the benzene ring for a thiophene ring in the central unit, like in the thienopyrazine (**TP-a**) and thienothiadiazole (**TT**) oligomers, causes a significant red shift. Extension of the parent thienopyrazine ring by fusion with naphthalene (**TP-b**) does not have a pronounced effect on the optical band gap, which is reduced by only 0.02 eV going from **TP-a** to **TP-b**. The naphthalene unit does create an enhanced absorption in the 400–500 nm region. Overall the band gap of these CPDT based oligomers can be by controlled over a 0.65 eV range by changing the central unit.

Triplet excited states and their energies

Triplet–triplet absorptions were investigated by near steady-state photoinduced absorption (PIA). Because formation of the triplet states of these oligomers by direct $S_1 \leftarrow S_0$ excitation, followed by intersystem crossing to T_1 was not successful, triplet states were populated by using [6,6]-phenyl-C₆₁-butyric acid methyl ester (PCBM) as a triplet sensitizer. In this experiment PCBM is excited by the laser and forms the triplet excited state with a quantum yield of about unity. The triplet energy can then be transferred to the oligomer, yielding the T_1 state of the oligomer and the S_0 ground state of PCBM, provided that the triplet energy of the oligomer is lower than that of PCBM. PIA spectra recorded for the oligomers in toluene in the presence of PCBM are depicted in Fig. 3.

For the oligomers with benzene-based acceptors, strong PIA signals are obtained, showing a $T_n \leftarrow T_1$ absorption band at



Scheme 1 Synthesis of the oligomers, R = 2-ethylhexyl.

1.72–1.92 eV and one or two vibronic peaks at higher energy. In addition, a number of weaker absorptions, extending to below 1 eV are present, showing that the dominant $T_n \leftarrow T_1$ absorption does not correspond to the lowest excited triplet state. The thiophene-based systems, which have smaller band gaps, show only very weak triplet absorptions. This is probably related to the reduced lifetime of the triplet excited states in these oligomers, because the triplet states are actually formed, evidenced by the almost complete quenching of the PCBM triplet (inset in Fig. 3b). The spectra of **TP-a** and **TP-b** also show two absorption peaks (one of which probably overlaps with the PCBM signal in

case of **TP-b**), located at higher energy than for the benzene-based acceptor systems. For **TT**, no triplet absorptions are observed at all, although the PCBM triplet is quenched completely, indicating triplet energy transfer to the oligomer.

To estimate the energy levels of the triplet excited states (E_T), quenching experiments have been performed. In these experiments, reference compounds with known triplet energy levels are added to the mixture. Depending on the relative triplet energies of the oligomer and reference compound, the triplet state of the oligomer is preserved or quenched. In the latter case the triplet of the reference will be detected. Fig. 4a shows the partial quenching

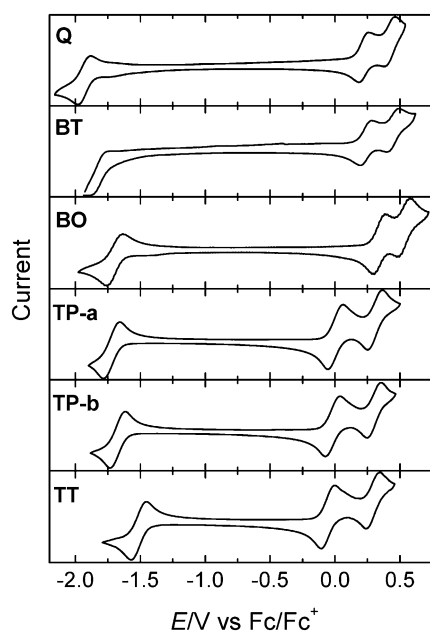


Fig. 1 Cyclic voltammograms of the oligomers in dichloromethane.

of the **BO** triplet by rubrene ($E_T = 1.14$ eV)⁴⁸ and the simultaneous formation of the rubrene signal at 2.48 eV. The fact that triplet absorptions of both compounds are visible at the same time indicates that both triplet states have very similar energies. The same experiment for **BT** gives a similar graph, for **Q** no quenching of the triplet signatures or appearance of the rubrene triplet absorption were observed. This leads to the conclusion that both **BT** and **BO** have $E_T \approx 1.14$ eV, while the triplet energy of **Q** is less than 1.14 eV. Quenching experiments of bis(trihexylsiloxy)silicon 2,3-naphthalocyanine ($E_T = 0.93$ eV)⁴⁹ with all oligomers result in the spectra shown in Fig. 4b. As expected **BT** and **BO** do not quench the naphthalocyanine triplet absorption, as their triplet energies of around 1.14 eV are well above the triplet energy of the naphthalocyanine. With **Q**, also no quenching of the naphthalocyanine triplet is observed, leading to the conclusion that the triplet energy of **Q** is higher than 0.93 eV. The thienopyrazines (**TP-a** and **TP-b**) partially quench the naphthalocyanine triplet, indicating that their triplet levels are located at about the same energy as the triplet level of naphthalocyanine (0.93 eV). **TT** quenches the naphthalocyanine somewhat more than the thienopyrazines, therefore its triplet level is estimated to be less than 0.9 eV.

The estimated triplet energy levels (E_T) are summarized in Table 1 together with the singlet–triplet splitting energy (ΔE_{ST})

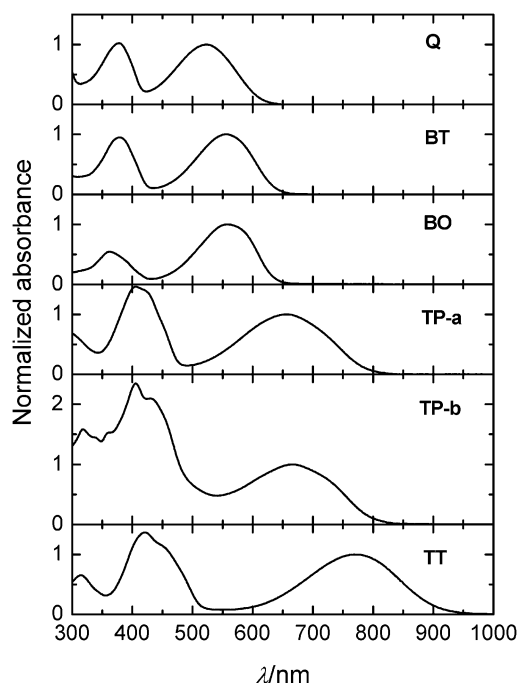


Fig. 2 Normalized UV/vis absorption spectra of the oligomers in toluene.

calculated using the optical band gaps ($\Delta E_{ST} = E_g^{opt} - E_T$). Bearing the experimental uncertainties in mind, there is a trend towards a reduced exchange energy with decreasing band gap.

Radical cations

Chemical oxidation of the oligomers was performed by adding a solution of thianthrenium hexafluorophosphate⁵⁰ to a solution of the oligomers in dichloromethane in small aliquots. UV/vis/NIR absorption spectra were obtained. The spectra for **BT** are shown in Fig. 5a, the other oligomers gave similar spectra.

Upon addition of thianthrenium hexafluorophosphate, the absorption band of the neutral oligomer disappears and two new bands at lower energy appear. These bands are attributed to the dipole-allowed $D_1 \leftarrow D_0$ and $D_2 \leftarrow D_0$ transitions of the doublet-state radical cation that, in first approximation, correspond to electron excitations from HOMO \rightarrow SOMO (singly occupied molecular orbital) and SOMO \rightarrow LUMO (see Fig. 5b). The energy maxima of these absorptions are summarized in Table 1. The position of these maxima does not show great variation upon changing the acceptor strength, with a $D_1 \leftarrow D_0$ transition around 0.8 eV (the only exception being the

Table 1 Experimental optical and electrochemical (vs. ferrocene) data for the oligomers

Oligomer	E_g^{opt} (eV)	E_{max}^{opt} (eV)	E_{ox} (V)	E_{red} (V)	E_g^{cv} (V)	$T_n \leftarrow T_1$ (eV)		$D_1 \leftarrow D_0$ (eV)	$D_2 \leftarrow D_0$ (eV)	E_T (eV)	ΔE_{ST} (eV)
Q	2.02	2.37	0.15	−1.86	2.01	1.72	1.88	0.80	1.45	0.93–1.14	1.0
BT	1.95	2.24	0.18	−1.73	1.91	1.74	1.90	0.82	1.40	1.14	0.8
BO	1.95	2.21	0.26	−1.63	1.89	1.82	1.98	0.81	1.33	1.14	0.8
TP-a	1.57	1.89	−0.07	−1.64	1.57	1.92	2.29	1.02	1.35	0.93	0.6
TP-b	1.55	1.86	−0.10	−1.60	1.50	—	2.22	1.04	1.36	0.93	0.6
TT	1.37	1.61	−0.13	−1.44	1.31	—	—	0.77	1.32	<0.9	>0.5

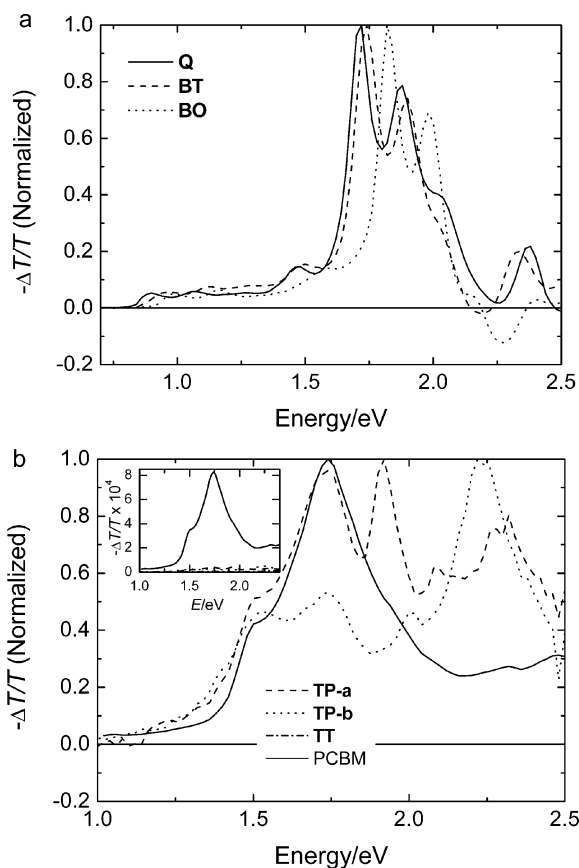


Fig. 3 Normalized PIA spectra of the oligomers (0.1 mM) in toluene in the presence of PCBM (0.4 mM): benzene-based acceptors (a) and thiophene-based acceptors (b). As a reference, the normalized PIA spectrum of PCBM is also shown in panel (b). The inset in panel (b) shows the unnormalized spectra, illustrating the quenching of the PCBM triplet.

thienopyrazines, which have this transition at about 1 eV) and a $D_2 \leftarrow D_0$ transition around 1.3–1.4 eV. This limited variation points to a localization of the excitations on the donor units of the oligomers, instead of a strong charge-transfer character of the absorption, as is observed when exciting the neutral oligomers.

Quantum-chemical calculations

The evolution of the electronic and optical properties of the oligomers upon variation of the acceptor unit has also been characterized at the theoretical level in order to provide a deeper insight into the experimental data. We have optimized the ground-state geometry of the six oligomers at the DFT level using the standard B3LYP functional and a 6–31G (d,p) basis set using the Gaussian 2003 package.⁵¹ The alkyl substituents have been replaced by hydrogen atoms and planarity has been imposed on the conjugated backbone. The geometry in the lowest triplet excited state has been optimized at the same level of theory, as motivated by the reliable triplet energies provided by this approach.⁵² The energy of the vertical $S_1 \leftarrow S_0$ transition, to be compared to the experimental E_{\max}^{opt} values, has been obtained by coupling the DFT approach to a time-dependent (TD) formalism; the energy of the fully relaxed S_1 state has been inferred by subtracting from the vertical transition energy the reorganization energy in the excited state; the latter is directly

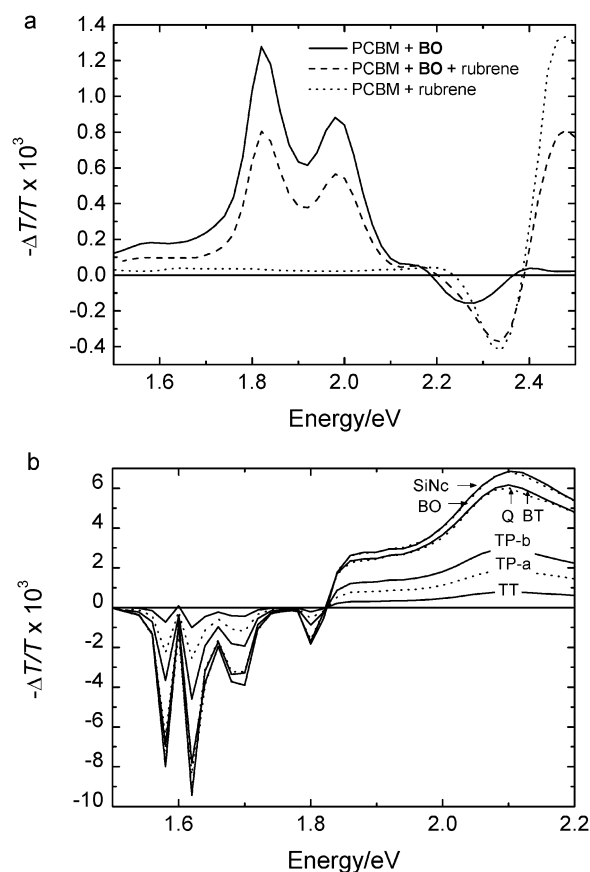


Fig. 4 Partial quenching of the **BO** triplet and formation of the rubrene triplet (a) and partial quenching of the bis(trihexylsiloxy)silicon 2,3-naphthalocyanine (SiNc) triplet by the oligomers containing thiophene-based acceptors, the benzene based acceptors show no quenching (b).

accessible from the experimental data as the energy difference between E_{\max}^{opt} and E_g^{opt} ($E_{\text{reorg}} = E_{\max}^{\text{opt}} - E_g^{\text{opt}}$). A summary of the theoretical data is given in Table 2.

The $S_1 \leftarrow S_0$ transition is mostly described for all oligomers by a HOMO to LUMO one-electron excitation. The calculated and experimental values of the vertical transition energies (E_{\max}) are plotted in Fig. 6a. The experimental evolution is reproduced very well, though the TD-DFT values underestimate E_{\max} by about 0.3 eV.⁵³ There is a drop in the lowest optical transition energy by 0.72 eV going from **Q** to **TT**, in full consistency with the experimental value of 0.65 eV. The calculated HOMO and LUMO levels are depicted in Fig. 6b together with the corresponding experimental oxidation and reduction potentials. This graph shows that the general experimental trends are once again reproduced very well. In particular, the calculations confirm that there is a marked increase in the HOMO energy when changing the acceptor from a benzene-based to a thiophene-based unit and that **BO** has the highest ionization potential. The results also rationalize the reduction of the band gap with the increase of the acceptor strength (**BT** and **BO** vs. **Q**, **TT** vs. **TP**), mainly due to stabilization of the LUMO. No conclusions can be made about the exact offsets between the calculated and experimental HOMO and LUMO levels, as the potential of Fc/Fc^+ vs. vacuum is set arbitrarily in Fig. 6b. This comparison is hampered by uncertainties in both the calculations and in the experimental

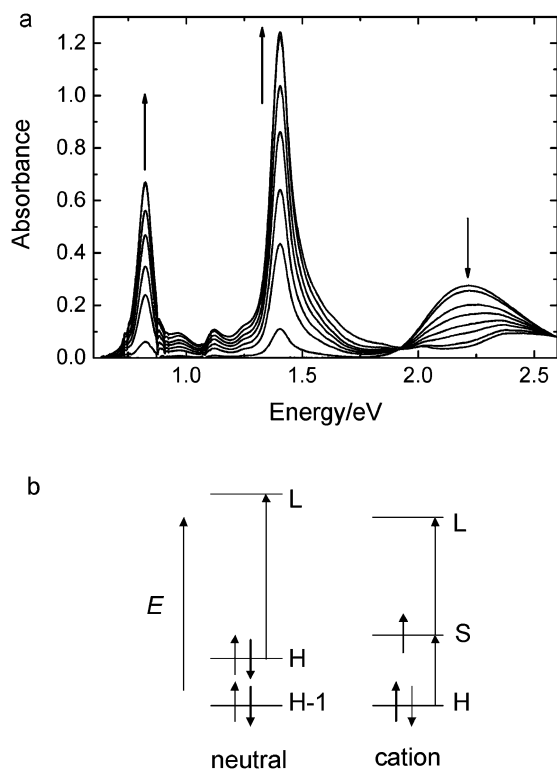


Fig. 5 (a) Chemical oxidation of **BO** with thianthrenium hexafluorophosphate in dichloromethane. The appearance and disappearance of bands is shown with arrows. (b) Schematic orbital diagram for the main dipole-allowed transitions of the neutral oligomer and the radical cation, H = HOMO S = SOMO and L = LUMO.

determination of the electrochemical potential of the Fc/Fc^+ redox couple vs. vacuum.^{54,55}

Table 2 shows that in the oligomers with a thiophene-based acceptor (**TP-a**, **TP-b**, **TT**), the HOMO is more or less delocalized evenly over the entire molecule since the distribution over the donor and acceptor units is close to the statistical expectation of $\sim 70\%$ and $\sim 30\%$, respectively, which follows from simply counting the sp^2 hybridized atoms on the donor and acceptor parts (neglecting the naphthalene unit in **TP-b** which does not affect the band gap according to Table 1). For the oligomers containing a benzene-based acceptor, the HOMO gets localized in a more pronounced way on the donor units. The larger delocalization in the thiophene-based acceptors is consistent with the higher HOMO levels calculated and measured for these systems.

Table 2 Calculated HOMO/LUMO energies, distribution of these orbitals over the donor (D) and acceptor (A) parts calculated from the LCAO (linear combination of atomic orbitals) coefficients, $S_1 \leftarrow S_0$ and $T_n \leftarrow T_1$ transition energies, energies of the lowest triplet state in the fully relaxed geometry (E_T), and energy difference between the lowest fully relaxed singlet versus triplet excited states (ΔE_{ST})

Oligomer	HOMO (eV)	LUMO (eV)	Distribution HOMO		Distribution LUMO		E_{max}			
			D (%)	A (%)	D (%)	A (%)	$S_1 \leftarrow S_0$ (eV)	$T_n \leftarrow T_1$ (eV)	E_T (eV)	ΔE_{ST} (eV)
Q	-4.69	-2.34	80	20	33	67	2.06	1.96	1.23	0.48
BT	-4.74	-2.68	78	22	34	66	1.90	2.05	0.93	0.68
BO	-4.84	-2.64	79	21	35	65	1.99	2.08	1.02	0.72
TP-a	-4.48	-2.61	71	29	32	68	1.66	2.00	0.66	0.68
TP-b	-4.40	-2.50	68	32	30	70	1.66	2.15	0.75	0.60
TT	-4.40	-2.93	69	31	27	73	1.34	2.35	0.31	0.79

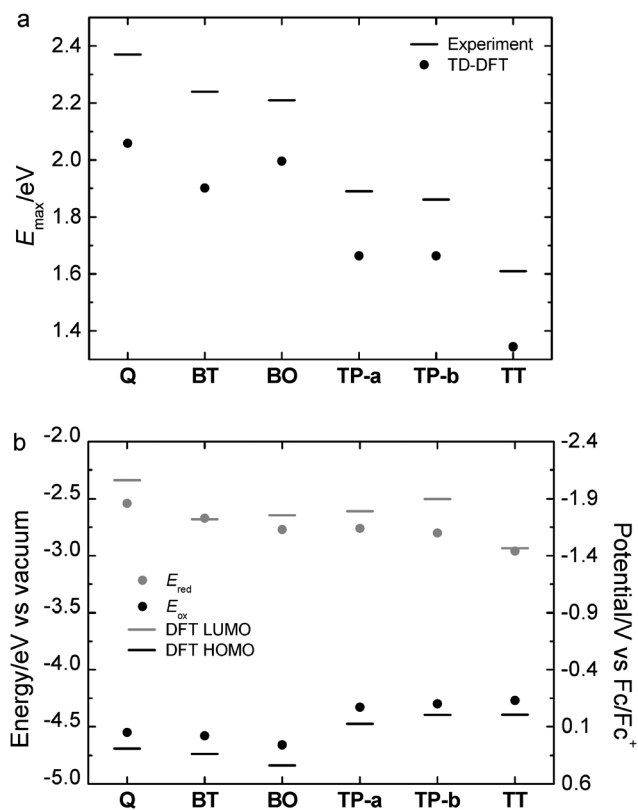


Fig. 6 Theoretical and experimental vertical transition energies (a) and calculated frontier orbital energies and measured redox potentials (b). Values calculated at the DFT level are depicted as horizontal bars and experimental values by dots.

Table 2 further indicates that the LUMO is located mostly on the acceptor unit for all oligomers (by 68% on average). Among the various molecules, the differences between the distribution of the LUMO level are less pronounced than for the HOMO level, although the LUMO becomes somewhat more confined on the acceptor unit for the strongest acceptor (**TT**).

The calculated triplet $T_n \leftarrow T_1$ absorption energies are fairly close to the experimental values while a larger discrepancy is observed for the lowest triplet energies (E_T) (Fig. 7a). The latter can be attributed in part to the experimental uncertainties in determining the triplet energy levels by quenching experiments though this cannot reconcile all differences between experiment and theory, in particular the relative order of **Q** and **BT**. The experimentally determined triplet energies are in a quite narrow

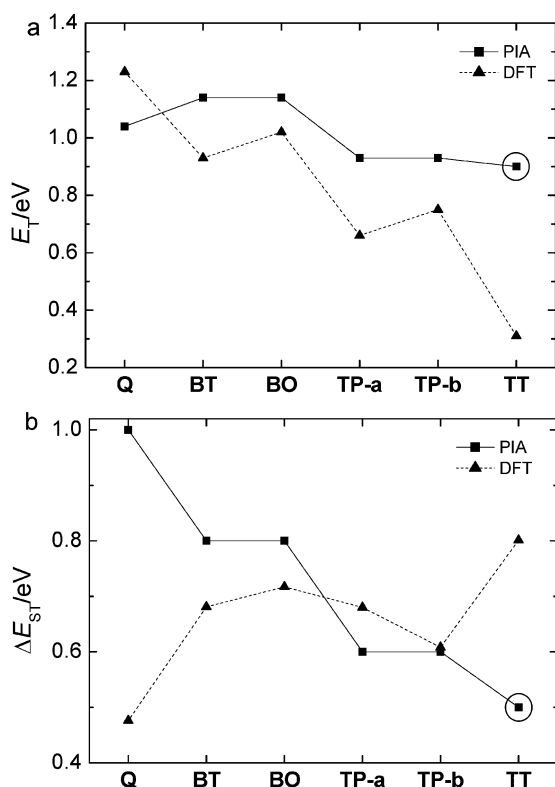


Fig. 7 (a) Experimental and calculated triplet energies E_T (a) and singlet–triplet energy splitting ΔE_{ST} (b). The experimental value of E_T for **TT** (circled entries) is an upper limit, so that the corresponding ΔE_{ST} is a lower limit.

range (0.90–1.14 eV) while the calculated values show a much stronger variation with the choice of the acceptor. The calculated value for the triplet energy of the thienothiadiazole oligomer of 0.3 eV is very low for an electronically excited state; we stress, however, that the experimental value of 0.9 eV can only be considered as an upper limit in this case.

The calculated singlet–triplet energy splittings $\Delta E_{ST} = E_{\max} - E_{\text{reorg}} - E_T$ are compared to the experimental values in Fig. 7b. While the experimentally determined ΔE_{ST} shows a clear decrease with increasing acceptor strength, the calculated values do not show a clear trend and changes are sometimes opposite to the experimental observations. Similarly, large ΔE_{ST} values (between 0.6 and 0.8 eV) are obtained at both the theoretical and experimental levels for **BT**, **BO**, **TP-a**, and **TP-b**. A larger discrepancy is observed for **Q** while the comparison for **TT** is hampered by the uncertainty in the experimental E_T value.

ΔE_{ST} reflects the exchange energy, which at first approximation is determined by the extent to which the HOMO and LUMO levels share the same regions of space. Naively, one might expect that by introducing stronger acceptor units, the exchange energy is reduced because the LUMO would get more strongly confined on the acceptor and the HOMO on the donor. In fact, this expectation seems to coincide with the experimental trend for ΔE_{ST} shown in Fig. 7b. However, by inspecting the contributions of the donor and acceptor units over the frontier orbitals (Table 2), there is fairly little variation among the oligomers. The calculated values do not show any appreciable trend, strongly suggesting that changes in ΔE_{ST} are determined by more subtle

effects that go beyond the simple rationale mentioned above. In fact, the molecule with the strongest acceptor (**TT**) is predicted to have the largest ΔE_{ST} value.

Conclusions

Oligomers consisting of two cyclopentadithiophene units and six different electron-deficient aromatic ring systems have been prepared. The influence of the acceptor on the optical and electrochemical properties has been investigated both experimentally and theoretically on the basis of density functional theory calculations. The experimental values for optical and electrochemical band gaps are almost similar and fully supported by (TD-)DFT calculations that show a similar evolution of the lowest singlet transition energy compared to experiments and a good correlation between the calculated energies of the frontier electronic levels and the experimental redox potentials.

The optical band gap of the oligomers changes from 1.4 to 2 eV depending on the acceptor as a consequence of substantial changes in both the oxidation *and* reduction potentials, because the HOMO is delocalized over the entire molecule while the LUMO is mainly localized on the acceptor. The optical absorption spectra of the radical cations of the oligomers show little variation when changing the acceptors, suggesting that the electronic structures are dominated by the cyclopentadithiophene units. Triplet absorption spectra and triplet energies have been determined from near steady-state PIA experiments using triplet quenchers. Experimentally estimated values lead to triplet energies that are relatively constant, between <0.9 and 1.14 eV. DFT predicts much larger variations from 1.23 eV for **Q**, going down to a value as low as 0.66 eV for **TP-a**, and 0.31 eV for **TT**. The low triplet energies might cause charge recombination into a triplet state to become an important loss mechanism in the application of small band gap materials in organic solar cells. Predicting or rationally controlling the exchange energy in these small band gap systems by simple arguments is presently not possible.

Acknowledgements

The research was supported by a TOP grant of the Chemical Sciences (CW) division of the Netherlands Organization for Scientific Research (NWO) and is part of the Joint Solar Programme (JSP). The JSP is co-financed by the Foundation for Fundamental Research on Matter (FOM), Chemical Sciences of NWO, and the Foundation Shell Research. The joint collaboration is supported by the European Commission through the Human Potential Program Marie-Curie Research Training Network NANOMATCH (Grant No. MRTN-CT-2006-035884). The work in Mons is further supported by the Belgian National Fund for Scientific Research (FNRS). J.C. is a research fellow of FNRS. J.G. is a ‘Ramón y Cajal’ Research Fellow, financed by the Spanish Ministry for Education and Science.

References

- 1 F. Padinger, R. S. Rittberger and N. S. Sariciftci, *Adv. Funct. Mater.*, 2003, **13**, 85.

- 2 G. Li, V. Shrotriya, J. Huang, Y. Yao, T. Moriarty, K. Emery and Y. Yang, *Nat. Mater.*, 2005, **4**, 864.
- 3 M. D. Irwin, D. B. Buchholz, A. W. Hains, R. P. H. Chang and T. J. Marks, *Proc. Natl. Acad. Sci. U. S. A.*, 2008, **105**, 2783.
- 4 C. Winder and N. S. Sariciftci, *J. Mater. Chem.*, 2004, **14**, 1077.
- 5 A. Dhanabalan, J. K. J. van Duren, P. A. van Hal, J. L. J. van Dongen and R. A. J. Janssen, *Adv. Funct. Mater.*, 2001, **11**, 255.
- 6 X. J. Wang, E. Perzon, J. L. Delgado, P. de la Cruz, F. L. Zhang, F. Langa, M. Andersson and O. Inganas, *Appl. Phys. Lett.*, 2004, **85**, 5081.
- 7 L. M. Campos, A. Tontcheva, S. Gunes, G. Sonmez, H. Neugebauer, N. S. Sariciftci and F. Wudl, *Chem. Mater.*, 2005, **17**, 4031.
- 8 M. M. Wienk, M. G. R. Turbiez, M. P. Struijk, M. Fonrodona and R. A. J. Janssen, *Appl. Phys. Lett.*, 2006, **88**, 153511.
- 9 F. Zhang, W. Mammo, L. M. Andersson, S. Admassie, M. R. Andersson and O. Inganas, *Adv. Mater.*, 2006, **18**, 2169.
- 10 Y. Zhu, R. D. Champion and S. A. Jenekhe, *Macromolecules*, 2006, **39**, 8712.
- 11 D. Mühlbacher, M. Scharber, M. Morana, Z. G. Zhu, D. Waller, R. Gaudiana and C. Brabec, *Adv. Mater.*, 2006, **18**, 2884.
- 12 M. M. Wienk, M. P. Struijk and R. A. J. Janssen, *Chem. Phys. Lett.*, 2006, **422**, 488.
- 13 E. Perzon, F. L. Zhang, M. Andersson, W. Mammo, O. Inganas and M. R. Andersson, *Adv. Mater.*, 2007, **19**, 3308.
- 14 J. Peet, J. Y. Kim, N. E. Coates, W. L. Ma, D. Moses, A. J. Heeger and G. C. Bazan, *Nat. Mater.*, 2007, **6**, 497.
- 15 M. M. Wienk, M. Turbiez, J. Gilot and R. A. J. Janssen, *Adv. Mater.*, 2008, **20**, 2556.
- 16 J. Hou, H. Y. Chen, S. Zhang, G. Li and Y. Yang, *J. Am. Chem. Soc.*, 2008, **130**, 16144.
- 17 F. Wudl, M. Kobayashi and A. J. Heeger, *J. Org. Chem.*, 1984, **49**, 3382.
- 18 I. Hoogmartens, P. Adriaenssens, D. Vanderzande, J. Gelan, C. Quattrocchi, R. Lazzaroni and J. L. Brédas, *Macromolecules*, 1992, **25**, 7347.
- 19 M. Pomerantz, B. Chaloner-Gill, L. O. Harding, J. J. Tseng and W. J. Pomerantz, *J. Chem. Soc., Chem. Commun.*, 1992, 1672–1673.
- 20 J. P. Niefeld, C. L. Heth and S. C. Rasmussen, *Chem. Commun.*, 2008, 981–983.
- 21 M. S. Taylor and T. M. Swager, *Angew. Chem., Int. Ed.*, 2007, **46**, 8480.
- 22 H. Reisch, U. Wiesler, U. Scherf and N. Tuytuylikov, *Macromolecules*, 1996, **29**, 8204.
- 23 C. Kitamura, S. Tanaka and Y. Yamashita, *Chem. Mater.*, 1996, **8**, 570.
- 24 J. Roncali, *Chem. Rev.*, 1997, **97**, 173.
- 25 H. A. M. van Müllekom, J. A. J. M. Vekemans, E. E. Havinga and E. W. Meijer, *Mater. Sci. Eng., R*, 2001, **32**, 1.
- 26 E. Bundgaard and F. C. Krebs, *Sol. Energy Mater.*, 2007, **91**, 954.
- 27 J. Mei, N. C. Heston, S. V. Vasilyeva and J. R. Reynolds, *Macromolecules*, 2009, **42**, 1482.
- 28 T. T. Steckler, X. Zhang, J. Hwang, R. Honeyager, S. Ohira, X. H. Zhang, A. Grant, S. Ellinger, S. A. Odom, D. Sweat, D. B. Tanner, A. G. Rinzler, S. Barlow, J. L. Brédas, B. Kippelen, S. R. Marder and J. R. Reynolds, *J. Am. Chem. Soc.*, 2009, **131**, 2824.
- 29 T. T. Steckler, K. A. Abboud, M. Craps, A. G. Rinzler and J. R. Reynolds, *Chem. Commun.*, 2007, 4904.
- 30 H. A. Becerril, N. Miyaki, M. L. Tang, R. Mondal, Y. S. Sun, A. C. Mayer, J. E. Parmer, M. D. McGehee and Z. Bao, *J. Mater. Chem.*, 2009, **19**, 591.
- 31 X. Guo and M. D. Watson, *Org. Lett.*, 2008, **10**, 5333.
- 32 N. Blouin, A. Michaud, D. Gendron, S. Wakim, E. Blair, R. Neagu-Plesu, M. Belletete, G. Durocher, Y. Tao and M. Leclerc, *J. Am. Chem. Soc.*, 2008, **130**, 732.
- 33 N. Blouin, A. Michaud and M. Leclerc, *Adv. Mater.*, 2007, **19**, 2295.
- 34 M. Zhang, H. N. Tsao, W. Pisula, C. D. Yang, A. K. Mishra and K. Mullen, *J. Am. Chem. Soc.*, 2007, **129**, 3472.
- 35 Z. Zhu, D. Waller, R. Gaudiana, M. Morana, D. Mühlbacher, M. Scharber and C. Brabec, *Macromolecules*, 2007, **40**, 1981.
- 36 B. Pal, W.-C. Yen, J.-S. Yang, C.-Y. Chao, Y.-C. Hung, S.-T. Lin, C.-H. Chuang, C.-W. Chen and W.-F. Su, *Macromolecules*, 2008, **41**(18), 6664–6671.
- 37 A. J. Moulé, A. Tsami, T. W. Buennagel, M. Forster, N. M. Kronenberg, M. Scharber, M. Koppe, M. Morana, C. J. Brabec, K. Meerholz and U. Scherf, *Chem. Mater.*, 2008, **20**, 4045.
- 38 S. Xiao, H. Zhou and W. You, *Macromolecules*, 2008, **41**, 5688.
- 39 J. Hou, T. L. Chen, S. Zhang, H.-Y. Chen and Y. Yang, *J. Phys. Chem. C*, 2009, **113**, 1601.
- 40 B. P. Karsten, L. Viani, J. Gierschner, J. Cornil and R. A. J. Janssen, *J. Phys. Chem. A*, 2008, **112**, 10764.
- 41 B. P. Karsten and R. A. J. Janssen, *Org. Lett.*, 2008, **10**, 3513.
- 42 B. P. Karsten, L. Viani, J. Cornil, and R. A. J. Janssen, unpublished work.
- 43 T. A. Ford, I. Afilov, D. Beljonne and N. C. Greenham, *Phys. Rev. B*, 2005, **71**.
- 44 T. Offermans, P. A. van Hal, S. C. J. Meskers, M. M. Koetse and R. A. J. Janssen, *Phys. Rev. B*, 2005, **72**.
- 45 T. A. Ford, H. Ohkita, S. Cook, J. R. Durrant and N. C. Greenham, *Chem. Phys. Lett.*, 2008, **454**, 237.
- 46 A. P. Monkman, H. D. Burrows, L. J. Hartwell, L. E. Horsburgh, I. Hamblett and S. Navaratnam, *Phys. Rev. Lett.*, 2001, **86**, 1358.
- 47 A. Kohler and D. Beljonne, *Adv. Funct. Mater.*, 2004, **14**, 11.
- 48 W. G. Herkstroeter and P. B. Merkel, *J. Photochem.*, 1981, **16**, 331.
- 49 P. A. Firey, W. E. Ford, J. R. Sounik, M. E. Kenney and M. A. J. Rodgers, *J. Am. Chem. Soc.*, 1988, **110**, 7626.
- 50 H. J. Shine, B. J. Zhao, J. N. Marx, T. Ould-Ely and K. H. Whitmire, *J. Org. Chem.*, 2004, **69**, 9255.
- 51 *Gaussian 03, Revision C.02*, M. J. Frisch, G. W. Trucks, H. B. Schlegel, G. E. Scuseria, M. A. Robb, J. R. Cheeseman, J. A. Montgomery, Jr., T. Vreven, K. N. Kudin, J. C. Burant, J. M. Millam, S. S. Iyengar, J. Tomasi, V. Barone, B. Mennucci, M. Cossi, G. Scalmani, N. Rega, G. A. Petersson, H. Nakatsuji, M. Hada, M. Ehara, K. Toyota, R. Fukuda, J. Hasegawa, M. Ishida, T. Nakajima, Y. Honda, O. Kitao, H. Nakai, M. Klene, X. Li, J. E. Knox, H. P. Hratchian, J. B. Cross, V. Bakken, C. Adamo, J. Jaramillo, R. Gomperts, R. E. Stratmann, O. Yazyev, A. J. Austin, R. Cammi, C. Pomelli, J. W. Ochterski, P. Y. Ayala, K. Morokuma, G. A. Voth, P. Salvador, J. J. Dannenberg, V. G. Zakrzewski, S. Dapprich, A. D. Daniels, M. C. Strain, O. Farkas, D. K. Malick, A. D. Rabuck, K. Raghavachari, J. B. Foresman, J. V. Ortiz, Q. Cui, A. G. Baboul, S. Clifford, J. Cioslowski, B. B. Stefanov, G. Liu, A. Liashenko, P. Piskorz, I. Komaromi, R. L. Martin, D. J. Fox, T. Keith, M. A. Al-Laham, C. Y. Peng, A. Nanayakkara, M. Challacombe, P. M. W. Gill, B. Johnson, W. Chen, M. W. Wong, C. Gonzalez, and J. A. Pople, Gaussian, Inc., Wallingford CT, 2004.
- 52 D. Wasserberg, P. Marsal, S. C. J. Meskers, R. A. J. Janssen and D. Beljonne, *J. Phys. Chem. B*, 2005, **109**, 4410.
- 53 This is due to the inherent overestimation of long range interactions of standard functionals (without or with small HF exchange like B3LYP). This is already quite pronounced for the size of oligomers considered here, *i.e.* 5 rings, see *e.g.* J. Gierschner, J. Cornil and H.-J. Egelhaaf, *Adv. Mater.*, 2007, **19**, 173. However, different oligomers can be well compared if they have a similar conjugation length as is the case here.
- 54 J. O. Bockris and S. U. M. Khan, *Surface Electrochemistry: A Molecular Level Approach*, Kluwer Academic/Plenum Publishers, New York, 1993.
- 55 V. V. Pavlishchuk and A. W. Addison, *Inorg. Chim. Acta*, 2000, **298**, 97.